Published in final edited form as:
Brain. 2005 July ; 128(Pt 7): 1498–1510. doi:10.1093/brain/awh510.

Cell type analysis of functional fetal dopamine cell suspension transplants in the striatum and substantia nigra of patients with Parkinson's disease

Ivar Mendez[1], **Rosario Sanchez-Pernaute**[3], **Oliver Cooper**[3], **Angel Viñuela**[3], **Daniela Ferrari**[3], **Lars Björklund**[3], **Alain Dagher**[2], and **Ole Isacson**[3]

1*Dalhousie University and Queen Elizabeth II Health Science Center, Division of Neurosurgery and Neuroscience, Halifax*

2*McGill University and Montreal Neurological Institute, McConnel Brain Imaging Centre, Montreal, Canada*

3*Harvard University and McLean Hospital, NINDS Udall Parkinson's Disease Research Center of Excellence, Belmont, MA, USA*

Abstract

We report the first post-mortem analysis of two patients with Parkinson's disease who received fetal midbrain transplants as a cell suspension in the striatum, and in one case also in the substantia nigra. These patients had a favourable clinical evolution and positive ^{18}F-fluorodopa PET scans and did not develop motor complications. The surviving transplanted dopamine neurons were positively identified with phenotypic markers of normal control human substantia nigra ($n = 3$), such as tyrosine hydroxylase, G-protein-coupled inward rectifying current potassium channel type 2 (Girk2) and calbindin. The grafts restored the cell type that provides specific dopaminergic innervation to the most affected striatal regions in the parkinsonian brain. Such transplants were able to densely reinnervate the host putamen with new dopamine fibres. The patients received only 6 months of standard immune suppression, yet by post-mortem analysis 3–4 years after surgery the transplants appeared only mildly immunogenic to the host brain, by analysis of microglial CD45 and CD68 markers. This study demonstrates that, using these methods, dopamine neuronal replacement cell therapy can be beneficial for patients with advanced disease, and that changing technical approaches could have a favourable impact on efficacy and adverse events following neural transplantation.

Keywords

transplantation; dopamine neuron; Parkinson's disease

Introduction

The degeneration and loss of a specific neuronal cell population in the ventral midbrain leads to the development of Parkinson's disease (Marsden, 1994). These midbrain neurons modulate motor function through dopamine innervation of basal ganglia and forebrain regions. Pharmacological substitution of dopamine produces remarkable benefits for some years but is hampered by complications as the disease progresses (Marsden, 1994; Rajput *et al*., 2002). A more ambitious approach aims to restore function by replacement of the dopamine neurons

Correspondence to: Professor Ole Isacson, Neuroregeneration Laboratory, Harvard Medical School, McLean Hospital, MRC 130, 115 Mill St, Belmont, MA 02478, USA, E-mail: isacson@hms.harvard.edu.

and their connections by fetal or stem cells. Transplanted human fetal ventral midbrain neurons have shown functional capacity (Lindvall *et al*., 1990, 1994; Freed *et al*., 1992, 2001; Peschanski *et al*., 1994; Hauser *et al*., 1999; Piccini *et al*., 1999, 2000; Mendez *et al*., 2002), but also side-effects in some patients (Freed *et al*., 2001; Olanow *et al*., 2003). Previous reports of post-mortem analysis of transplanted Parkinson's disease patients were from patients receiving solid ventral midbrain donor tissue pieces. These reports showed evidence of survival and partial reinnervation of the host brain (Kordower *et al*., 1995, 1996; Freed *et al*., 2001; Olanow *et al*., 2003). There have been no prior post-mortem studies of cases where cells are first dissociated and isolated using proteolytic enzymes, then counted and prepared for transplantation as a cell suspension into the brain (Bjorklund *et al*., 1983).

The ectopic placement of fetal cells in the striatum may also contribute to limited functional effects of transplants. At least in rodent models, grafts placed both in the striatum and substantia nigra (SN) improve the recovery in complex behavioural tasks (Baker *et al*., 2000; Mukhida *et al*., 2001) compared with intrastriatal grafts alone. In an effort to optimize the functional benefit of fetal transplantation, we started a safety and feasibility pilot study in Halifax, Canada, to evaluate simultaneous intrastriatal and intranigral grafts (Mendez *et al*., 2002), and one of the patients reported here had received cells both into the midbrain and into the striatum.

The human ventral midbrain contains several functional subpopulations of dopamine neurons that can be identified by both specific biochemical markers and connectivity to their target neurons (Gerfen *et al*., 1985, 1987; Lynd-Balta and Haber, 1994). In order to define the dopamine neural subtypes we analysed specific markers of human adult ventral midbrain neurons projecting to either motor or limbic areas. Identification of cell-specific (phenotypic) markers of this subpopulation is relevant for both cell replacement and neuroprotective therapies (Bjorklund and Isacson, 2002). Calbindin is expressed in dopamine neurons projecting to the limbic nucleus accumbens region and is not expressed in cells projecting to the dorsolateral motor putamen (Gerfen *et al*., 1985; Haber *et al*., 1995; Liang *et al*., 1996; Hontanilla *et al*., 1997; Nemoto *et al*., 1999). Calbindin-positive dopamine neurons are relatively spared in Parkinson's disease (Yamada *et al*., 1990; Fearnley and Lees, 1991; German *et al*., 1992; Gibb, 1992; Damier *et al*., 1999) and in toxic (1-methyl-4-phenyl-1,2,3,6-tetrahydropyridine; MPTP) and genetic (weaver mouse) models (Graybiel *et al*., 1990; Gaspar *et al*., 1994). The weaver phenotype in mice, in which 50% of the dopamine neurons degenerate in the first postnatal weeks (Bayer *et al*., 1995) and all surviving dopamine neurons express calbindin (Gaspar *et al*., 1994), is caused by a mutation in the G-protein-coupled inward rectifying current potassium channel type 2 (Girk2). Girk2 tetramers are almost exclusively expressed in the membrane of dopamine neurons projecting to the dorsolateral putamen and are functionally linked to dopamine D2 and $GABA_B$ receptors (Inanobe *et al*., 1999; Guatteo *et al*., 2000).

Our focus in this report is on the specific cellular and morphological variables that may be relevant to the functional effects observed in patients. A better understanding of the cellular identities, growth and graft–host interaction of fetal ventral midbrain transplants is required to develop a rational basis for the use of fetal nigral or other cell sources, such as stem cells, for future therapies.

Patients and methods

Patient selection

The inclusion criteria for selecting these patients included a diagnosis of idiopathic Parkinson's disease, made independently by two neurologists, and preoperative PET imaging consistent with Parkinson's disease. The patients responded well to levodopa from the onset of the disease, but the maximum tolerated medication did not provide adequate relief of symptoms and caused

unacceptable side-effects. The patients had a detailed assessment for at least 6 months prior to surgery, as defined by the validated Core Assessment Program for Intracerebral Transplantation (CAPIT) (Langston *et al*., 1992). Pre- and post-operative clinical assessment was performed on an outpatient basis at regular intervals using the Unified Parkinson's Disease Rating Scale (UPDRS) (Fahn and Elton, 1987). A timed motor task of hand pronation/supination (15 s) was also used. All tests were done at maximum on/off periods as defined by the CAPIT protocol. Video recordings were assessed by blinded observers. The patients and their caregivers maintained diaries throughout the trial that included a registry of medication. The patients were screened for serological evidence of infection and exposure to syphilis, hepatitis B and C, HIV, cytomegalovirus (CMV) and human T-cell lymphotrophic virus using the standard automated immunoassays (Abbott AxSYM, Abbott Park, IL, USA) at Queen Elizabeth Hospital (Halifax, CA, USA). CMV-negative patients never received tissue from CMV-positive donors.

Cell suspension preparation

Fetal ventral midbrain tissue was collected with maternal consent from HIV, hepatitis B and C, human T-cell lymphotrophic virus, and syphilis-negative women undergoing elective abortion between 6 and 9 weeks after conception, in the pregnancy termination unit of our centre under the strict guidelines of a protocol approved by the university and hospital ethical review boards. Embryo staging was confirmed by ultrasound evaluation of length and external features corresponding to Carnegie stages 17–21 (6–9 weeks) (O'Rahilly and Muller, 1987). Fetal ventral midbrains were dissected under sterile conditions and tissue samples of each specimen were sent for aerobic and anaerobic culture. The ventral midbrains (three or four per procedure) were minced in several small pieces and stored for 6 days at 4°C in 2 ml of a low-sodium, phosphate-buffered, calcium-free hibernation medium with glial-derived neurotrophic factor (GDNF; 1 μg per ml hibernation medium; Pepro Tech, Rocky Hill, NJ, USA) (Mendez *et al*., 2000b). Cell suspensions of ventral midbrain tissue were incubated in 0.1% trypsin/0.05% DNase/Dulbecco's modified Eagle medium (DMEM) (trypsin; Worthington, Freehold, NJ, USA) (DNase/DMEM; Sigma, Chicago, IL, USA) at 37°C for 20 min, then rinsed four times in 0.05% DNase/DMEM. The tissue was then mechanically dissociated using successively smaller sterilized micropipettes until a quasi-single-cell suspension was achieved. This cell suspension was not completely homogeneous and contained small aggregates of cells. A final cell concentration of approximately 80 000/μl was used, with a viability of 99%, as determined by the trypan blue dye exclusion method.

Transplantation procedures

The surgical transplantation procedures were performed in two stages 4 weeks apart. On the day of surgery, each patient was fitted with a Leksell stereotactic headframe (Elekta, Stockholm, Sweden) under local anaesthesia. The stereotactic coordinates for targets in the postcommissural putamen were calculated using T1- and T2-weighted MRI images and a computerized stereotactic planning workstation (Surgiplan; Elekta) (Mendez *et al*., 2002). Transplantation was performed with the patient under local anaesthesia and sedation using a combination of midazolam (0.25–1.0 mg bolus doses) and propofol (10–20 mg bolus followed by infusion at 15–40 μg/kg/min). In patient 1, a burr-hole was placed at the level of the coronal suture (2 cm laterally) and a customized transplantation cannula (Mendez *et al*., 2000b) was inserted into four different targets approximately 3 mm apart in the postcommissural putamen. A 50 μl Hamilton syringe, fitted with a custom-made microinjector (Mendez *et al*., 2000b), was used to load the cell suspension in the transplantation cannula. The cell suspension was deposited along each of four putaminal trajectories previously calculated on the patient's MRI scan. The patient received 1 g of Ancel (Cefazolin sodium, QELI Hospital, Halifax, Canada) intravenously before the skin incision was made and three more doses of 1 g of Ancef intravenously every 8 h postoperatively. The patient had an MRI (General Electric; Signa

Horizon 1.0 T MRI, T1 and T2 axial, coronal and sagittal images) 24 h after surgery and was discharged from the hospital 48 h after surgery.

Patient 2 received first a deposit in the midbrain at the level of the dorsorostral SN (Mendez *et al*., 2002) and six in the striatum, two of them oriented from caudate to putamen (transventricular) and the other four as described above. Cell preparation and targeting were done in the same way described for patient 1. Four weeks later the patient underwent a second procedure that was not completed due to a small bleeding apparent through the cannula after the first putaminal deposit. This bleeding was not apparent in the MRI performed 24 h later.

The patients received immunosuppressive medication (cyclosporin A, 5–8 mg/kg/day) beginning 2 weeks prior to admission. Doses were tapered to 2 mg/kg/day and continued for 6 months. Immunosuppressive doses were adjusted on the basis of serum levels to be in the range of 150–200 μg/l. Renal function was monitored closely to prevent immunosuppressive toxicity. Postoperatively, every effort was made to keep antiparkinsonian medications at their preoperative level and modifications were only made on clinical grounds.

Imaging studies

PET scans were performed preoperatively and at regular intervals after surgery at the McConnell Brain Imaging Centre (Montreal Neurological Institute, McGill University) on a Siemens ECAT HR+ PET in 3D mode, with a resolution of approximately 5 mm full width at half maximum (FWHM) in all directions at the centre of the field of view. On the day of the study, the patient did not receive antiparkinsonian medications. One hour prior to the scan, a peripheral inhibitor of aromatic amino acid decarboxylase (carbidopa, 150 mg orally) was administered to prevent the peripheral breakdown of ^{18}F-fluorodopa (^{18}F-DOPA). The head was immobilized within the aperture of the PET scanner by a form-fitting vacuum device. The patient received 3–5 mCi of ^{18}F-DOPA as a bolus injection into the antecubital vein over 2 min and data were acquired for 90 min in 27 time frames of increasing duration. PET images were automatically realigned to MRI images for each patient (Mendez *et al*., 2002). MRI scans were transformed into standardized stereotactic space (Mendez *et al*., 2002). Then, regions of interest were drawn onto the MRI in stereotactic space on the basal ganglia and cerebellum. The cerebellum was used as a reference region to calculate the ^{18}F-DOPA uptake constant (K_i) using the graphical method of Patlak and Blasberg (1985). In addition, K_i maps were generated by calculating the uptake constant at each voxel and constants were taken of the areas of interest.

Autopsy and tissue preparation

For both Parkinson's disease patients, the brains were infused, after a 3–4 h post-mortem delay, with 2 l of cold 0.1 M phosphate buffer, pH 7.4 followed by 2 l of ice-cold paraformaldehyde in 0.1 M phosphate buffer. The brains were subsequently blocked in the coronal plane in 3 cm thick slabs. The slabs were cryoprotected in 30% sucrose in phosphate-buffered saline (PBS) at 4°C until they were completely submerged. Coronal sections (40 μm) were cut serially on a Leitz freezing microtome and stored until histological analysis in Millonig's solution (6% azide in 0.1 M phosphate buffer). In order to determine the normal dopamine neuronal distribution and cell type (subpopulation)-specific markers, we obtained postfixed midbrain blocks from three age-matched control brains that had no brain pathology recorded on autopsy. This human control tissue was obtained from the Neuropathology Division at Brigham and Women's Hospital, Harvard Medical School, Boston.

Immunohistochemistry and stereological procedures

Sections (40 μm) were stained by immunohistochemistry using either immunoperoxidase or immunofluorescence techniques. Sections for immunoperoxidase staining were treated for 30

min in 3% hydrogen peroxide (Humco, Texarkana, TX, USA), washed three times in PBS, and incubated in 10% normal goat serum (Vector Laboratories, Burlingame, CA, USA) and 0.1% Triton X-100 in PBS for 60 min prior to overnight incubation at 4°C with the primary antibody [rabbit anti-tyrosine hydroxylase (TH); Pel Freez, Rogers AK, 1 : 300; rabbit anti-GFAP (glial fibrillary acidic protein); Dako, Denmark, 1 : 500; mouse anti-CD68 and anti-CD4-5; Dako, Denmark, 1 : 500 and 1 : 100, respectively] in 2% normal goat serum and 0.1% Triton X-100. After three 10-min rinses in PBS, the sections were incubated in biotinylated secondary antibody (goat anti-rabbit/mouse; Vector Laboratories, Burlingame, CA, USA, 1 : 300) diluted in 2% normal goat serum in PBS at room temperature for 60 min. The sections were rinsed three times in PBS and incubated in streptavidin–biotin complex (Vectastain ABC Elite Kit; Vector Laboratories) in PBS for 60 min at room temperature. Following thorough rinsing with PBS, staining was visualized by incubation in 3,3′-diaminobenzidine solution and intensified with nickel (Vector Laboratories). On selected sections, the primary antibody was omitted to verify specific staining. Sections were counterstained with cresyl violet to place the immunostain into cellular context. After immunostaining, floating tissue sections were mounted on Superfrost Plus glass slides (Fisher Scientific, Pittsburgh, PA, USA), dehydrated, cleared and coverslipped. For immunofluorescence, sections were rinsed for 3 × 10 min in PBS, incubated in 10% normal donkey serum (Vector Laboratories) and 0.1% Triton X-100 in PBS for 60 min and then incubated overnight at room temperature in primary antibody (sheep anti-TH; Pel Freez, Rogers, AK, 1 : 300; rabbit anti-Girk2; Alomone Laboratories, Jerusalem, Israel, 1 : 80; anti-calbindin; Swant, Bellinzona, Switzerland, 1 : 2000). After an additional three 10-min rinses in PBS the sections were incubated in fluorescent dye-conjugated secondary antibodies (Alexa Fluor donkey anti-rabbit/mouse/sheep 488/568/660; Molecular Probes, Eugene, OR, USA; 1 : 500) in PBS with 10% normal donkey serum for 60 min at room temperature. After rinsing in PBS (3 × 10 min), sections were mounted onto Superfrost Plus slides and coverslipped in Gel/Mount (Biomeda Corporation, Foster City, CA, USA). Sections were examined using a confocal microscope (LSM510 Meta; Carl Zeiss, Thornwood, NY, USA). Design-based stereology was performed on the specimens using an integrated brightfield microscope (Axioskop 2; Carl Zeiss), confocal microscope (LSM510) and StereoInvestigator image capture equipment and software (MicroBrightField, Williston, VT, USA). Graft volumes and TH-positive cell counts were calculated using the Cavalieri estimator probe and optical fractionator probe, respectively, from one-sixth of the total sections. The coefficient of error was used to assess probe accuracy and $P < 0.05$ was considered acceptable. The 3D reconstruction was created from one-sixth of the total sections using Neurolucida solid modelling software (MicroBrightField). The graft constituent cell ratios were calculated by two investigators independently counting cells in several (20–30) randomly selected high power fields. The images were captured by confocal microscopy and colocalization was confirmed by *z*-axis analysis. Maps of Girk2-, calbindin- and TH-expressing and coexpressing cell distributions were created from transverse serial sections of normal human midbrain stained for TH and each of the other markers by double immunofluorescence. These maps were generated using Stereo-Investigator. Cell soma diameter was measured using the same software on random sections in the striatal and midbrain grafts and control tissue. An average of 100 cells was measured and group sizes were compared using analysis of variance (Statview software, SAS Institute, Cary, NC, USA).

Results

Survival and integration of dopamine neurons transplanted as cell suspensions in the striatum of patients with Parkinson's disease

Patient 1—The patient was a 69-year-old man with a 15-year history of Parkinson's disease who underwent bilateral transplantation (4 weeks apart) of fetal ventral midbrain cell suspensions. A total of 3.2×10^6 cells from three donors (40 μl) were implanted along four

tracks in the right postcommissural putamen and 2.6×10^6 cells from two donors (32 μl) in the left side. The patient experienced a gradual clinical improvement that started 3–4 months after transplantation. The preoperative and last postoperative (3-year follow-up) UPDRS scores are shown in Table 1A. While levodopa doses were kept unchanged, dyskinesia scores also improved (Table 1A) and he never experienced off-period dyskinesia. Two years and 4 months after transplantation, a PET study showed an increase in ^{18}F-DOPA uptake bilaterally (Table 1A, Fig. 1) more pronounced in the right putamen, reaching 88% of normal Ki values for the right side and 65% for the left side (normal average ^{18}F-DOPA Ki = 0.008). Three years and 8 months after transplantation, the patient suffered an acute myocardial infarct and died in the coronary intensive care unit. Permission for an autopsy had been obtained and the brain was retrieved for histological analysis. The presence of Lewy bodies in the substantia nigra confirmed the diagnosis of Parkinson's disease.

Macroscopically, TH-positive grafts were observed along the four surgical cell infusion tracks (Fig. 2) in the putamen regions of both hemispheres. The surviving cell suspension grafts were slender in shape and did not displace the host putamen (Fig. 2). The grafts extended through the major axis of the putamen in dorsocaudal and mediolateral trajectories (as seen in 3D reconstructions; Fig. 2). TH staining demonstrated that all four graft sites contained numerous dopamine neurons (Fig. 2). Using stereological methods, the graft volumes and dopamine cell numbers were quantified (Table 2). The total number of dopamine neurons on the right side was found to be 127 189 (Table 2). They were distributed along the four surgical tracks (anterior to posterior, as shown in Fig. 2D). Surviving dopamine neurons per track were: track 1 = 51 206; track 2 = 36 340; track 3 = 38 935; and track 4 = 708 (track 4 was the last cell infusion site). On the left side, a total of 98 913 dopamine neurons were distributed in the four tracks (Fig. 2): track 1, 10 383; track 2, 56 869; track 3, 20 294 and track 4, 11 367. Surviving dopamine neurons typically formed clusters in the outer segments of the aggregated cellular deposits (Fig. 2). Immediately adjacent to the graft, dopamine donor axons had a similar density to that found in normal striatum (Fig. 2). Further away (10–15 mm), the TH fibre density appeared less than in spared regions of the caudate. Most dopamine neurons in the graft were melanized (data not shown). The glial content was estimated using antibodies against GFAP (for astrocytes) and CD45 and CD68 (for microglia/macrophages). The morphology of astrocytes (Fig. 4H) around and inside the grafts was not markedly different from that in host areas away from the graft, or normal patient control brain regions. Around the perimeter of the grafts, there were many typical fibrous type 1 astrocytes and some thicker astrocyte branches. The typical appearance of resting microglia was seen throughout the host brain (Fig. 4K). This unreactive morphology of microglia was also found around and inside the grafts. Few macrophages and activated microglia were found in grafted regions, along the needle tracks only (Fig. 4I).

Patient 2—The patient was a 59-year-old woman with an 11-year history of Parkinson's disease, who received bilateral multiple-site transplantation. In the first procedure, cells from four donors were implanted in the right substantia nigra (500 000 cells in one track) and in the caudate putamen (four tracks in the putamen and two tracks tangentially oriented from caudate to putamen; Fig. 3), giving a total of ~4.8 million cells. In the left hemisphere, 6 weeks later, she received cells from three donors in the nigra (one track, 500 000 cells) and in the putamen (one track, 800 000 cells). The procedure for the left hemisphere was not completed due to bleeding through the cannula after the first putaminal deposit. The patient showed no neurological deficit related to the complication during surgery. The patient showed a progressive improvement of parkinsonian signs, and L-dopa treatment was decreased by 30%. The patient showed a remarkable improvement in total and motor UPDRS scores (~50%; Table 1B) and in quality of life, in spite of the severity of the disease at the time of the surgical intervention. The improvement was marked on the left side while at 3 years parkinsonian signs had continued to worsen on the right side (Table 1B), which was initially the less affected side of the body. At this post-transplantation time, a ^{18}F-DOPA PET study (Fig. 3A) showed a

marked increase in the right putamen and further loss of signal in the left putamen (Table 1B). The patient died 4 years and 4 months after transplantation from unrelated causes: acute renal failure, possibly due to an underlying renal cell carcinoma (autopsy permission was restricted to the brain).

Post-mortem analysis showed that the right putamen was densely and almost completely reinnervated, in contrast to the severe loss of TH-immunoreactive fibres in the left putamen, where there was no graft survival. In the left hemisphere we did not identify any graft, transplanted dopamine neuron or abnormal histology (no haemosiderin), except a minor (150 μm in diameter), glial GFAP-positive scar at the ventral base of the putamen. In contrast, in the right striatum, five grafts along the six tracks were identified (Fig. 3C). A total of 202 933 TH-positive cells (Table 2) were distributed as follows: track 1, 29 024; track 2, 25 956; tracks 3–4, 94 152; track 5, 45 542; and track 6, 8 259. The average diameter of the dopamine neurons in the grafts was 37 ± 1 μm. The orientation of the tracks is schematically shown in Fig. 3C. The TH neurons were aggregated in the periphery of the deposits and extended processes into the host striatum (Fig. 4A–D). The thick TH neurites in and around the deposits became arborized and reinnervated the entire putamen to nearly normal levels and, to a lesser extent, the caudate nucleus. No TH neurons were found in the left putamen, where TH fibre loss was very severe (Fig. 4E). Around the grafts there was a concentric area (~ 0.2–0.4 mm) where GFAP-positive fibres were oriented in fascicles (Fig. 4F–G) but did not prevent robust outgrowth of TH neurites. In this area, CD45-positive cell density appeared to be slightly higher than inside the graft (Fig. 4 J) but macrophages and activated cells were present only along needle tracks. In most brain areas, including the grafted regions, microglial cells show typical resting morphology (inset in Fig. 4K).

Analysis of dopamine neuron subpopulations in the normal human midbrain and in cell suspension transplants

In order to be able to selectively label different neuronal cell types and distinguish them in the patient's dopamine cellular grafts, we first performed a study of dopamine neuronal subpopulations in the normal human midbrain (n = 3). We mapped the distribution of two markers that have been reported (in different species) to be differentially expressed in dopamine neurons projecting to the motor striatum and nucleus accumbens/limbic areas: calbindin and Girk2. We found that dopamine neurons coexpressing calbindin (Fig. 5) were predominantly located in the retrorubral field (A8), the dorsal and lateral parts of the substantia nigra pars compacta (SNc, A9) and the ventral tegmental area (VTA, A10), excluding the most lateral division of this nucleus (paranigral and parabrachialis). We next determined the expression of Girk2. In the human control ventral midbrain, the distribution of TH/Girk2 immunoreactive neurons and neuropil was restricted to the ventral tier of the SNc (Fig. 5). In the putaminal cell suspension grafts (Table 2) we found a high proportion of Girk2 expression in TH neurons, with and without calbindin coexpression, which was consistent between grafts sites: in patient 1, 71% of dopamine neurons in the right and 69% in the left putamen, and in patient 2, 68% in the right-side caudate-putamen had the Girk2 staining typical of the ventral tier of SNc. Calbindin coexpression in dopamine neurons in the grafts was lower (~40%) than Girk2 expression, and more variable (26–48% colabelled with TH; Table 2). Therefore, we performed a subsequent analysis to map the distribution of the Girk2/TH neurons in representative graft deposits from both patients (Fig. 6). We consistently found that dopamine neurons in the outer perimeter of the graft deposits coexpressed Girk2 (Fig. 6A and B) while in the centre of the grafts the TH neurons were more often Girk2-negative (either calbindin-positive or both calbindin- and Girk2-negative).

Midbrain graft

The second patient also received an intranigral graft. The ^{18}F-DOPA PET study showed an increase in Ki values (but see the Discussion) in the right midbrain (Table 1B). Macroscopic examination revealed two small deposits in the right midbrain, between the rostral substantia nigra and the red nucleus (Fig. 7A). No grafts were identified on the left side. In the right midbrain, the parallel deposits extended in a rostrocaudal direction along the injection tract (Fig. 7B). A total of 4289 TH-positive cells were present in these grafts (Table 2). This represents 4–8% dopamine neuron survival, in contrast with 15–30% survival in the putaminal deposits (assuming a 5–10% dopamine content in the fetal midbrain preparation). The dopamine cells were located in the periphery of the deposits (Fig. 7C–F) and fewer TH-labelled neurons coexpressed Girk2 (Table 2, Fig. 7G–H) than seen in the putaminal grafts. As for the striatal locations, there was no lipofuscin inside the graft, which allowed a clear delineation of the graft perimeter using fluorescence microscopy. In addition, dopamine neurons inside the grafts were smaller than surrounding host neurons (mean diameter was 20.5 ± 1.2 μm in the graft and 46 ± 1.8 μm in the substantia nigra; $P < 0.0001$) and had less melanin (Fig. 7D–F). The distribution of TH/Girk2-positive neurons inside the graft was less clearly defined (Fig. 7I). There was no major microglial reaction in the host tissue. Most microglial cells (CD45 or CD68) showed resting morphology with only mild reaction around needle tracks, comparable to the observations in all grafts located in the striatum (Fig. 4I–K).

Discussion

This is the first post-mortem study of the survival and integration of cell-suspension human dopamine neuron grafts in Parkinson's disease patients. The fetal dopamine neurons transferred in a cell suspension and surviving in the striatum and substantia nigra had phenotypic markers of dopamine cell types expressed in normal ventral midbrain, a majority of them being calbindin-negative and expressing Girk2. Based on the data obtained in control human substantia nigra, we conclude that dopamine neurons with high expression of Girk2 and absence of calbindin correspond to ventrally located dopamine neurons that have been shown to project to the motor striatum (Gerfen *et al*., 1985; Lynd-Balta and Haber, 1994). This dopamine neuron type is selectively lost in Parkinson's disease. This is an important demonstration because it signifies that the appropriate dopamine ventral midbrain neuron types survive, grow and reinnervate the host putamen in Parkinson's disease patients, with long-term (more than 3 years) function without side-effects. This is also the first analysis of a cellular graft placed in the substantia nigra in a patient. The functional benefit observed in these patients, together with the absence of side-effects, in particular dyskinesias, is encouraging. The use of cell suspensions may cause less side-effects than other methods since 90% of patients receiving cell suspension grafts did not show off-phase dyskinesias (Hagell *et al*., 1999; Lindvall and Hagell, 2000; Mendez *et al*., 2002). In some of these patients there is evidence of physiological graft function beyond 11 years, as determined by dopamine release and activation of motor circuitry associated with a marked improvement in UPDRS and ratings of parkinsonism (Piccini *et al*., 1999, 2000). As previously reported for solid grafts (Kordower *et al*., 1995), survival of fetal cells in striatal grafts was correlated with enhancement of ^{18}F-DOPA uptake in the PET studies. In patient 1 there was restoration of ^{18}F-DOPA uptake to 88% of normal values in the right putamen and 65% in the left putamen. Similar results were observed in the right putamen of the second patient, while the specific uptake dropped further by another 45% by that time in the left side, where no grafted neurons survived. The annual loss of ^{18}F-DOPA uptake in parkinsonian patients in the posterior putamen has been estimated to be around 10% (Nurmi *et al*., 2001). In this patient there was a moderate increase in uptake in the midbrain (Table 1B). However, the significance of ^{18}F-DOPA uptake in the midbrain is complicated due to several factors, including a much lower normal uptake than in the striatum (Ki ~ 0.004), activity originating in neighbouring hindbrain serotonergic cell groups, and the small volume

of the region of interest (therefore vulnerable to partial volume effects, which increase the measurement error).

In these patients, the number of surviving dopamine neurons in the striatum is slightly higher than those published in recent studies (Freed *et al*., 2001; Olanow *et al*., 2003). Although a direct comparison of cell numbers between studies cannot be made because actual cell numbers grafted cannot be counted for technical reasons using solid fetal pieces, more TH-positive neurons survived in these grafts for the same number of donor embryos (30 000–50 000 per donor) than in solid grafts grafted as tissue strands or 'noodles' (~15 000; Freed *et al*., 2001), while the numbers were similar to those in patients transplanted with solid tissue pieces [30 000–50 000 (Kordower *et al*., 1996) and ~25 000 (Olanow *et al*., 2003)]. It has been demonstrated previously that preincubation with GDNF sustains and enhances dopamine neuron survival (Granholm *et al*., 1997; Espejo *et al*., 2000) and phenotypic gene expression (Costantini *et al*., 1997; Yurek and Fletcher-Turner, 1999) and increases neurite extension of fetal dopamine cells *in vitro* placed in the adult brain (Costantini and Isacson, 2002; Mendez *et al*., 2002). Current transplantation techniques use human fetal ventral midbrain obtained from elective abortions of donors 6–9 weeks after conception, when the dopamine cells are born but have not yet extended neurites. For these patients, we incubated the fetal ventral midbrain in GDNF and hibernation medium for 6 days prior to surgery, based on our previous laboratory and clinical studies (Apostolides *et al*., 1996; Rosenblad *et al*., 1996; Mehta *et al*., 1998; Mendez *et al*., 2000a; Hebb *et al*., 2003). Intriguingly, survival of dopamine neurons in the midbrain placement (from the same cell preparation) was lower (about 4–8%) in this patient, suggesting that differences may exist in survival depending on regional factors and conditions. We also observed that the cell body size of the surviving dopamine neurons placed in the midbrain in this case was significantly smaller than in the putamen and the host substantia nigra.

Our results contrast somewhat with the solid tissue transplantation methods that have been shown to be of variable benefit to Parkinson's disease patients (Freed *et al*., 2001; Olanow *et al*., 2003), with better outcome reported for patients with less severe UPDRS scores. In fact, in Olanow's study only patients with UPDRS motor score below 50 showed a treatment effect. These two patients experienced a consistent clinical improvement (~50%), including a reduction in the frequency and severity of dyskinesias in the on state and did not present dyskinesias in the off state. It is worth noting that the UPDRS scores in the off state improved close to 50% also in patient 2, demonstrating that dopamine cell therapy can be beneficial in patients with advanced disease at the time of the intervention, and suggests that differences in technical approaches could have an impact on clinical outcome.

Major differences are also observed between cell suspension and solid grafts with respect to angiogenesis (linked to immunogenicity), integration and the disruption of host histoarchitecture, and interaction and connectivity with host cells (Finsen *et al*., 1991; Geny *et al*., 1994; Leigh *et al*., 1994; Isacson *et al*., 1998). The neural macroscopic integration of the fetal ventral midbrain cell suspension implants in the Parkinson's disease patients' striatum reported here was noteworthy. The grafts had a slender shape and a smaller host tissue volume displacement than observed for solid tissue pieces in previous studies (Freed *et al*., 2001; Kordower *et al*., 1995, 1996). In the Parkinson's disease patients reported here, immune suppression therapy was withdrawn at 6 months, so consequently they had been without immunosuppression for ~ 3 years. The graft effects, PET scans and histology are consistent with the PET and clinical outcome of other Parkinson's disease patients that have received cell suspension grafts (Lindvall *et al*., 1994; Hagell *et al*., 1999; Mendez *et al*., 2002). We noted only minimal microglial activation and host tissue reaction to the grafts, using specific immunocytochemical markers. This is in contrast to reports of MHC II (major histocompatibility complex II) upregulation and microglial reactions to surviving solid ventral

midbrain grafts in Parkinson's disease patients (Kordower *et al*., 1997; Freed *et al*., 2001). In summary, the cell suspension grafts integrated well with the host, as has been shown previously in animal studies using cell suspension grafts (Nikkah *et al*., 1994), and had a minimal microglial activation, which is in contrast to what happened when solid tissue pieces were used, causing more severe microglial and immunological reactions in both patients (Kordower *et al*., 1997; Freed *et al*., 2001; and see figures in Olanow *et al*., 2003), and animal studies (Leigh *et al*., 1994). Several factors, including vascularization, trophic factor support and graft–host interaction, may be different for single cell suspension grafts and tissue pieces (Leigh *et al*., 1994; Nikkah *et al*., 1994). Transplantation antigens, such as MHC I, have one of their highest concentrations and levels in the body on endothelial cells and blood vessels (Finsen *et al*., 1991). Cell suspension grafts have a lower number of immunogenic graft-derived blood vessels than solid tissue grafts that eventually supply the surviving cells. Thus, instead host-derived angiogenic processes appear to dominate in cell suspension grafts (Peschanski and Isacson, 1988; Geny *et al*., 1994; Leigh *et al*., 1994).

By quantitative stereology in these transplants, we consistently found between 40 and 60% calbindin-negative and Girk2-positive dopamine neurons. There are also about 40–50% of Girk2-positive dopamine neurons in the dissected mammalian fetal midbrain (S.M. Chung and O. Isacson, unpublished observations). We further demonstrate that Girk2 is expressed in dopamine neurons of the adult human SNc (double-stained with TH), located in the ventral tier, and confirmed previous reports showing that ventrally located dopamine neurons do not coexpress calbindin. In rodents, Girk2 is expressed in SNc and in some TH-positive neurons in the most lateral groups of the ventral tegmental area (paranigralis and parabrachialis), and in the weaver mutation it is associated with about 50% loss of dopamine neurons (Schein *et al*., 1998). Our new data in the human brain (Fig. 5) show a predominant expression pattern of TH/Girk2 in dopamine neurons of the ventral SN. While Girk2 mutations have not yet been found in Parkinson's disease patients (Bandmann *et al*., 1998), Girk2 in its physiological role may contribute to the increased risk of damage or degeneration in dopamine neurons (Inanobe *et al*., 1999; Neuhoff *et al*., 2002). Interestingly, we found that the absence of calbindin and expression of Girk2 defines a ventral population of dopamine neurons that are known to project to motor areas of the putamen and are preferentially lost in Parkinson's disease. Our post-mortem analysis of the transplants shows a high proportion of TH/Girk2 coexpression in grafted dopamine neurons and a preferential distribution of these neurons at the graft–host interface in the striatum, with projections into their regular target of the host putamen. Experiments in rodents have demonstrated selective fibre outgrowth from subsets of mesencephalic dopamine neurons grafted in the cortex adjacent to the striatum (Schultzberg *et al*.,1984) or in the striatum (Haque *et al*., 1997), to their correct target, as shown also for other neuronal populations (Isacson and Deacon, 1996). These findings suggest the presence of appropriate neuron–target interactions in the adult brain that favour fibre outgrowth from the corresponding subset of dopamine neurons. The distribution of the TH/Girk2-positive neurons in the present grafts is an interesting finding in the light of the previous rodent and xenograft data (Isacson and Deacon, 1997), but more results will be needed to demonstrate the presence of such mechanisms in the adult human brain.

These analyses demonstrate the cellular composition, survival and integration of dopamine-containing suspension grafts in Parkinson's disease patients. These results also demonstrate that dopamine neuron replacement therapies can be effective in some patients even at advanced stages of the disease, and that changes in methodology may result in improved clinical outcome. Understanding specific cellular components of functional transplants may provide clues for effective cellular and synaptic restorative neurological therapies in the future.

Acknowledgements

This work was supported by the Canadian Institute of Health Research, Queen Elisabeth II Health Science Center (I.M.), National Institutes of Health (USA) NINDS Parkinson's Disease Research Center of Excellence (P50 NS 39793) (O.I.), The Harvard Center for Neurodegeneration and Repair, The Consolidated Anti-Aging Foundation and The Orchard Foundation.

References

Apostolides C, Sandford E, Hong M, Mendez I. Glial cell line-derived neurotrophic factor improves intrastriatal graft survival of stored dopaminergic cells. Neuroscience 1996;83:363–72. [PubMed: 9460746]

Baker KA, Sadi D, Hong M, Mendez I. Simultaneous intrastriatal and intranigral dopaminergic grafts in the parkinsonian rat model: role of the intranigral graft. J Comp Neurol 2000;426:106–16. [PubMed: 10980486]

Bandmann O, Marsden CD, Wood NW. Genetic aspects of Parkinson's disease. Mov Disord 1998;13:203–11. [PubMed: 9539331]

Bayer SA, Wills KV, Triarhou LC, Verina T, Thomas JD, Ghetti B. Selective vulnerability of late-generated dopaminergic neurons of the substantia nigra in weaver mutant mice. Proc Natl Acad Sci USA 1995;92:9137–40. [PubMed: 7568088]

Bjorklund L, Isacson O. Regulation of dopamine cell type and transmitter function in fetal and stem cell transplantation for Parkinson's disease. Prog Brain Res 2002;138:411–20. [PubMed: 12432781]

Bjorklund A, Stenevi U, Schmidt RH, Dunnett SB, Gage FH. Intracerebral grafting of neuronal cell suspensions. I. Introduction and general methods of preparation. Acta Physiol Scand Suppl 1983;522:1–7. [PubMed: 6586054]

Costantini, LC.; Isacson, O. Immunophilin ligands and dopamine neurons: specific effects in culture and in vivo. In: Borlongan, CV.; Isacson, O.; Sanberg, PR., editors. Immunosuppressant analogs in neuroprotection. Totowa, NJ: Humana Press; 2002. p. 49-66.

Costantini LC, Lin L, Isacson O. Medial fetal ventral mesencephalon: a preferred source for dopamine neuron grafts. Neuroreport 1997;8:2253–7. [PubMed: 9243621]

Damier P, Hirsch EC, Agid Y, Graybiel AM. The substantia nigra of the human brain. I. Nigrosomes and the nigral matrix, a compartmental organization based on calbindin D(28K) immunohistochemistry. Brain 1999;122:1421–36. [PubMed: 10430829]

Espejo M, Cutillas B, Arenas TE, Ambrosio S. Increased survival of dopaminergic neurons in striatal grafts of fetal ventral mesencephalic cells exposed to neurotrophin-3 or glial cell line-derived neurotrophic factor. Cell Transplant 2000;9:45–53. [PubMed: 10784066]

Fahn, S.; Elton, RL. Members of the UPDRS Development Committee. Unified Parkinson's Disease Rating Scale. New York, NY: Macmillan; 1987.

Fearnley JM, Lees AJ. Ageing and Parkinson's disease: substantia nigra regional selectivity. Brain 1991;114:2283–301. [PubMed: 1933245]

Finsen BR, Sorensen T, Castellano B, Pedersen EB, Zimmer J. Leukocyte infiltration and glial reactions in xenografts of mouse brain tissue undergoing rejection in the adult rat brain. A light and electron microscopical immunocytochemical study. J Neuroimmunol 1991;32:159–83. [PubMed: 1849517]

Freed CR, Breeze RE, Rosenberg NL, Schneck SA, Kriek E, Qi JX, et al. Survival of implanted fetal dopamine cells and neurologic improvement 12 and 46 months after transplantation for Parkinson's disease. N Engl J Med 1992;327:1549–55. [PubMed: 1435881]

Freed CR, Greene PE, Breeze RE, Tsai WY, DuMouchel W, Kao R, et al. Transplantation of embryonic dopamine neurons for severe Parkinson's disease. N Engl J Med 2001;344:710–9. [PubMed: 11236774]

Gaspar P, Ben Jelloun N, Febvret A. Sparing of the dopaminergic neurons containing calbindin-D28k and of the dopaminergic mesocortical projections in weaver mutant mice. Neuroscience 1994;61:293–305. [PubMed: 7969910]

Geny C, Naimi-Sadaoui S, Jeny R, Belkadi AM, Juliano SL, Peschanski M. Long-term delayed vascularization of human neural transplants to the rat brain. J Neurosci 1994;14:7553–62. [PubMed: 7996195]

Gerfen CR, Baimbridge KG, Miller JJ. The neostriatal mosaic: compartmental distribution of calcium-binding protein and parvalbumin in the basal ganglia of the rat and monkey. Proc Natl Acad Sci USA 1985;82:8780–4. [PubMed: 3909155]

Gerfen CR, Herkenham M, Thibault J. The neostriatal mosaic. II. Patch- and matrix-directed mesostriatal dopaminergic and non-dopaminergic systems. J Neurosci 1987;7:3915–34. [PubMed: 2891799]

German DC, Manaye KF, Sonsalla PK, Brooks BA. Midbrain dopaminergic cell loss in Parkinson's disease and MPTP-induced parkinsonism: sparing of calbindin-D28k-containing cells. Ann NY Acad Sci 1992;648:42–62. [PubMed: 1353337]

Gibb WR. Melanin, tyrosine hydroxylase, calbindin and substance P in the human midbrain and substantia nigra in relation to nigrostriatal projections and differential neuronal susceptibility in Parkinson's disease. Brain Res 1992;581:283–91. [PubMed: 1382801]

Granholm AC, Mott JL, Bowenkamp K, Eken S, Henry S, Hoffer BJ, et al. Glial cell line-derived neurotrophic factor improves survival of ventral mesencephalic grafts to the 6-hydroxydopamine lesioned striatum. Exp Brain Res 1997;116:29–38. [PubMed: 9305812]

Graybiel AM, Ohta K, Roffler-Tarlov S. Patterns of cell and fiber vulnerability in the mesostriatal system of the mutant mouse weaver. I. Gradients and compartments. J Neurosci 1990;10:720–33. [PubMed: 1690789]

Guatteo E, Fusco FR, Giacomini P, Bernardi G, Mercuri NB. The weaver mutation reverses the function of dopamine and GABA in mouse dopaminergic neurons. J Neurosci 2000;20:6013–20. [PubMed: 10934250]

Haber SN, Kunishio K, Mizobuchi M, Lynd-Balta E. The orbital and medial prefrontal circuit through the primate basal ganglia. J Neurosci 1995;15:4851–67. [PubMed: 7623116]

Hagell P, Schrag A, Piccini P, Jahanshahi M, Brown R, Rehncrona S, et al. Sequential bilateral transplantation in Parkinson's disease: effects of the second graft. Brain 1999;122:1121–32. [PubMed: 10356064]

Haque NS, LeBlanc CJ, Isacson O. Differential dissection of the rat E16 ventral mesencephalon and survival and reinnervation of the 6-OHDA-lesioned striatum by a subset of aldehyde dehydrogenase-positive TH neurons. Cell Transplant 1997;6:239–48. [PubMed: 9171157]

Hauser RA, Freeman TB, Snow BJ, Nauert M, Gauger L, Kordower JH, et al. Long-term evaluation of bilateral fetal nigral transplantation in Parkinson disease. Arch Neurol 1999;56:179–87. [PubMed: 10025423]

Hebb AO, Hebb K, Ramachandran AC, Mendez I. Glial cell line-derived neurotrophic factor-supplemented hibernation of fetal ventral mesencephalic neurons for transplantation in Parkinson disease: long-term storage. J Neurosurg 2003;98:1078–83. [PubMed: 12744369]

Hontanilla B, Parent A, Gimenez-Amaya JM. Parvalbumin and calbindin D-28k in the entopeduncular nucleus, subthalamic nucleus, and substantia nigra of the rat as revealed by double-immunohistochemical methods. Synapse 1997;25:359–67. [PubMed: 9097395]

Inanobe A, Yoshimoto Y, Horio Y, Morishige KI, Hibino H, Matsumoto S, et al. Characterization of G-protein-gated K+ channels composed of Kir3.2 subunits in dopaminergic neurons of the substantia nigra. J Neurosci 1999;19:1006–17. [PubMed: 9920664]

Isacson O, Deacon T. Specific axon guidance factors persist in the adult rat brain as demonstrated by pig neuroblasts transplanted to the rat. Neuroscience 1996;75:827–37. [PubMed: 8951876]

Isacson O, Deacon TW. Neural transplantation studies reveal the brain's capacity for continuous reconstruction. Trends Neurosci 1997;20:477–82. [PubMed: 9347616]

Isacson, O.; Deacon, T.; Schumacher, JM. Immunobiology and neuroscience of xenotransplantation in neurological disease. In: Tuszynski, MH.; Kordower, JH., editors. CNS regeneration: basic science and clinical advances. San Diego: Academic Press; 1998. p. 365-87.

Kordower JH, Freeman TB, Snow BJ, Vingerhoets FJG, Mufson EJ, Sanberg PR, et al. Neuropathological evidence of graft survival and striatal reinnervation after the transplantation of fetal mesencephalic tissue in a patient with Parkinson's disease. N Engl J Med 1995;332:1118–24. [PubMed: 7700284]

Kordower JH, Rosenstein JM, Collier TJ, Burke MA, Chen E-Y, Li JM, et al. Functional fetal nigral grafts in a patient with Parkinson's disease: chemoanatomic, ultrastructural, and metabolic studies. J Comp Neurol 1996;370:203–30. [PubMed: 8808731]

Kordower JH, Styren S, Clarke M, DeKosky ST, Olanow CW, Freeman TB. Fetal grafting for Parkinson's disease: expression of immune markers in two patients with functional fetal nigral implants. Cell Transplant 1997;6:213–9. [PubMed: 9171154]

Langston JW, Widner H, Goetz CG, Brooks D, Fahn S, Freeman T, et al. Core assessment program for intracerebral transplantations (CAPIT). Mov Disord 1992;7:2–13. [PubMed: 1557062]

Leigh K, Elisevich K, Rogers KA. Vascularization and microvascular permeability in solid versus cell-suspension embryonic neural grafts. J Neurosurg 1994;81:272–83. [PubMed: 7517998]

Liang CL, Sinton CM, German DC. Midbrain dopaminergic neurons in the mouse: co-localization with calbindin-D28K and calretinin. Neuroscience 1996;75:523–33. [PubMed: 8931015]

Lindvall O, Hagell P. Clinical observations after neural transplantation in Parkinson's disease. Prog Brain Res 2000;127:299–320. [PubMed: 11142032]

Lindvall O, Brundin P, Widner H, Rehncrona S, Gustavii B, Frackowiak R, et al. Grafts of fetal dopamine neurons survive and improve motor function in Parkinson's disease. Science 1990;247:574–7. [PubMed: 2105529]

Lindvall O, Sawle G, Widner H, Rothwell JC, Bjorklund A, Brooks D, et al. Evidence for long-term survival and function of dopaminergic grafts in progressive Parkinson's disease. Ann Neurol 1994;35:172–80. [PubMed: 8109898]

Lynd-Balta E, Haber SN. The organization of midbrain projections to the striatum in the primate: sensorimotor-related striatum versus ventral striatum. Neuroscience 1994;59:625–40. [PubMed: 7516506]

Marsden CD. Problems with long-term levodopa therapy for Parkinson's disease. Clin Neuropharmacol 1994;17 Suppl 2:S32–44. [PubMed: 9358193]

Mehta V, Hong M, Spears J, Mendez I. Enhancement of graft survival and sensorimotor behavioral recovery in rats undergoing transplantation with dopaminergic cells exposed to glial cell line-derived neurotrophic factor. J Neurosurg 1998;88:1088–95. [PubMed: 9609305]

Mendez I, Dagher A, Hong M, Hebb A, Gaudet P, Law A, et al. Enhancement of survival of stored dopaminergic cells and promotion of graft survival by exposure of human fetal nigral tissue to glial cell line–derived neurotrophic factor in patients with Parkinson's disease. Report of two cases and technical considerations. J Neurosurg 2000a;92:863–9. [PubMed: 10794303]

Mendez I, Hong M, Smith S, Dagher A, Desrosiers J. Neural transplantation cannula and microinjector system: experimental and clinical experience. Technical note. J Neurosurg 2000b;92:493–9. [PubMed: 10701543]

Mendez I, Dagher A, Hong M, Gaudet P, Weerasinghe S, McAlister V, et al. Simultaneous intrastriatal and intranigral fetal dopaminergic grafts in patients with Parkinson disease: a pilot study. Report of three cases. J Neurosurg 2002;96:589–96. [PubMed: 11883846]

Mukhida K, Baker KA, Sadi D, Mendez I. Enhancement of sensorimotor behavioral recovery in hemiparkinsonian rats with intrastriatal, intranigral, and intrasubthalamic nucleus dopaminergic transplants. J Neurosci 2001;21:3521–30. [PubMed: 11331381]

Nemoto C, Hida T, Arai R. Calretinin and calbindin-D28k in dopaminergic neurons of the rat midbrain: a triple-labeling immunohistochemical study. Brain Res 1999;846:129–36. [PubMed: 10536220]

Neuhoff H, Neu A, Liss B, Roeper J. I(h) channels contribute to the different functional properties of identified dopaminergic subpopulations in the midbrain. J Neurosci 2002;22:1290–302. [PubMed: 11850457]

Nikkah G, Olsson M, Eberhard J, Bentlage C, Cunningham MG, Bjorklund A. A microtransplantation approach for cell suspension grafting in the rat Parkinson model: a detailed account of the methodology. Neuroscience 1994;53:57–72.

Nurmi E, Ruottinen HM, Bergman J, Haaparanta M, Solin O, Sonninen P, et al. Rate of progression in Parkinson's disease: a 6-[18F]fluoro-L-dopa PET study. Mov Disord 2001;16:608–15. [PubMed: 11481683]

O'Rahilly, R.; Muller, F. Developmental stages in human embryos: including a revision of Streeter's horizons and a survey of the Carnegie collection. Washington DC: Carnegie Institution of Washington; 1987.

Olanow CW, Goetz CG, Kordower JH, Stoessl AJ, Sossi V, Brin MF, et al. A double-blind controlled trial of bilateral fetal nigral transplantation in Parkinson's disease. Ann Neurol 2003;54:403–14. [PubMed: 12953276]

Patlak CS, Blasberg RG. Graphical evaluation of blood-to-brain transfer constants from multiple-time uptake data. J Cerebr Blood Flow Metab 1985;5:584–90.

Peschanski M, Isacson O. Fetal homotypic transplants in the excitotoxically neuron depleted thalamus. I Light microscopy. J Comp Neurol 1988;274:449–63. [PubMed: 3220970]

Peschanski M, Defer G, N'Guyen J, Ricolfi F, Monfort J, Remy P, et al. Bilateral motor improvement and alteration of L-dopa effect in two patients with Parkinson's disease following intrastriatal transplantation of fetal ventral mesencephalon. Brain 1994;117:487–99. [PubMed: 8032859]

Piccini P, Brooks DJ, Bjorklund A, Gunn RN, Grasby PM, Rimoldi O, et al. Dopamine release from nigral transplants visualized in vivo in a Parkinson's patient. Nat Neurosci 1999;2:1137–40. [PubMed: 10570493]

Piccini P, Lindvall O, Bjorklund A, Brundin P, Hagell P, Ceravolo R, et al. Delayed recovery of movement-related cortical function in Parkinson's disease after striatal dopaminergic grafts. Ann Neurol 2000;48:689–95. [PubMed: 11079531]

Rajput AH, Fenton ME, Birdi S, Macaulay R, George D, Rozdilsky B, et al. Clinical-pathological study of levodopa complications. Mov Disord 2002;17:289–96. [PubMed: 11921114]

Rosenblad C, Martinez-Serrano A, Bjorklund A. Glial cell line-derived neurotrophic factor increases survival, growth and function of intrastriatal fetal nigral dopaminergic grafts. Neuroscience 1996;75:979–85. [PubMed: 8938733]

Schein J, Hunter D, Roffler-Tarlov S. Girk2 expression in the ventral midbrain, cerebellum, and olfactory bulb and its relationship to the murine mutation weaver. Dev Biol 1998;204:432–50. [PubMed: 9882481]

Schultzberg M, Dunnett SB, Bjorklund A, Stenevi U, Hokfelt T, Dockray GJ, et al. Dopamine and cholecystokinin immunoreactive neurons in mesencephalic grafts reinnervating the neostriatum: evidence for selective growth regulation. Neuroscience 1984;12:17–32. [PubMed: 6146944]

Yamada T, McGeer PL, Baimbridge KG, McGeer EG. Relative sparing in Parkinson's disease of substantia nigra dopamine neurons containing calbindin-D28K. Brain Res 1990;526:303–7. [PubMed: 2257487]

Yurek DM, Fletcher-Turner A. GDNF partially protects grafted fetal dopaminergic neurons against 6-hydroxydopamine neurotoxicity. Brain Res 1999;845:21–7. [PubMed: 10529440]

Abbreviations

^{18}F-DOPA
: ^{18}F-fluorodopa

GDNF
: glial-derived neurotrophic factor

GFAP
: glial fibrillary acidic protein

Girk2
: G-protein-coupled inward rectifying current potassium channel type 2

PBS
: phosphate buffered saline

SN
: substantia nigra

SNc
: substantia nigra pars compacta

TH

tyrosine hydroxylase

UPDRS

Unified Parkinson's Disease Rating Scale

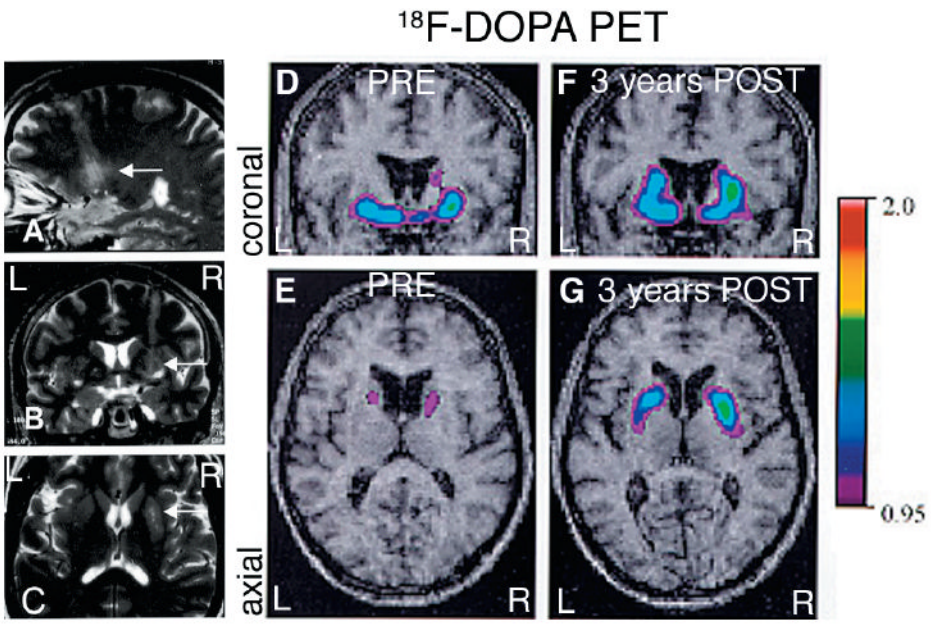

Fig. 1.

(**A**–**C**) MRI study performed 24 h after the first surgery (patient 1). The four parallel needle tracks through the right putamen are visible in the axial (**C**) and sagittal (**A**) views (compare with 3D reconstruction of the grafts in Fig. 2D). (**D**–**G**) Parametric maps of F-DOPA uptake (Ki) overlaid on the patient's MRI. (**D**–**E**) A preoperative PET scan showed a marked, asymmetrical decrease in putaminal ^{18}F-DOPA uptake in the first patient, consistent with the diagnosis of idiopathic Parkinson's disease. (**F**–**G**) Twenty-eight months after transplantation the PETs show a significant increase in ^{18}F-DOPA uptake, more pronounced in the right putamen (>300% compared with preoperative values) than on the left (100% increase). Ki values are included in Table 1A. R = right; L = left.

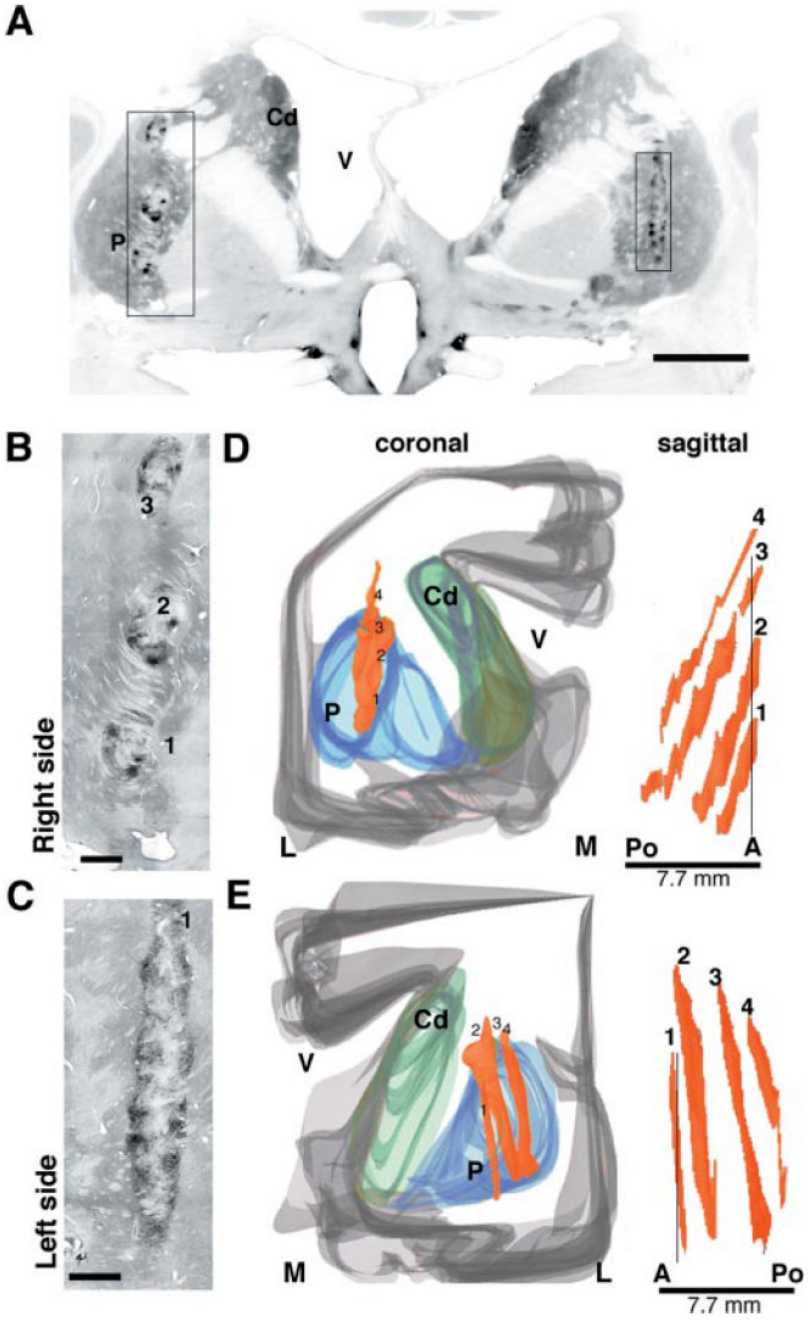

Fig. 2.

Morphological and cytoarchitectonic features of the cell suspension grafts in the putamen in patient 1. (**A**) Low-power microphotographs of TH immunostaining of a coronal section through the anterior portion of the grafts, at the level of the postcommissural putamen. (**B**) In the right putamen, clusters of TH-positive cells at the tip of three tracks are visible. (**C**) In the left hemisphere the cell infusion tracks are parallel to the section plane, so only the most anterior track is visible. TH-positive cells are predominantly located at the periphery of the grafts. (**D**–**E**) The spatial orientation of the grafts is demonstrated in the computer-assisted 3D reconstructions. This view shows the location of the grafts in the postcommissural putamen. The surviving cell aggregates spanned approximately 8 mm on the anterior–posterior axis in

both hemispheres and the trajectories are easily identified in the sagittal view. The four parallel grafts (1–4) are numbered in anterior–posterior order for stereological analyses (see text and Table 2). P = putamen; Cd = caudate nucleus; V = lateral ventricle; A = anterior; Po = posterior; M = medial; L = lateral. Scale bars: **A**, 1 cm; **B**, **C**, 1 mm.

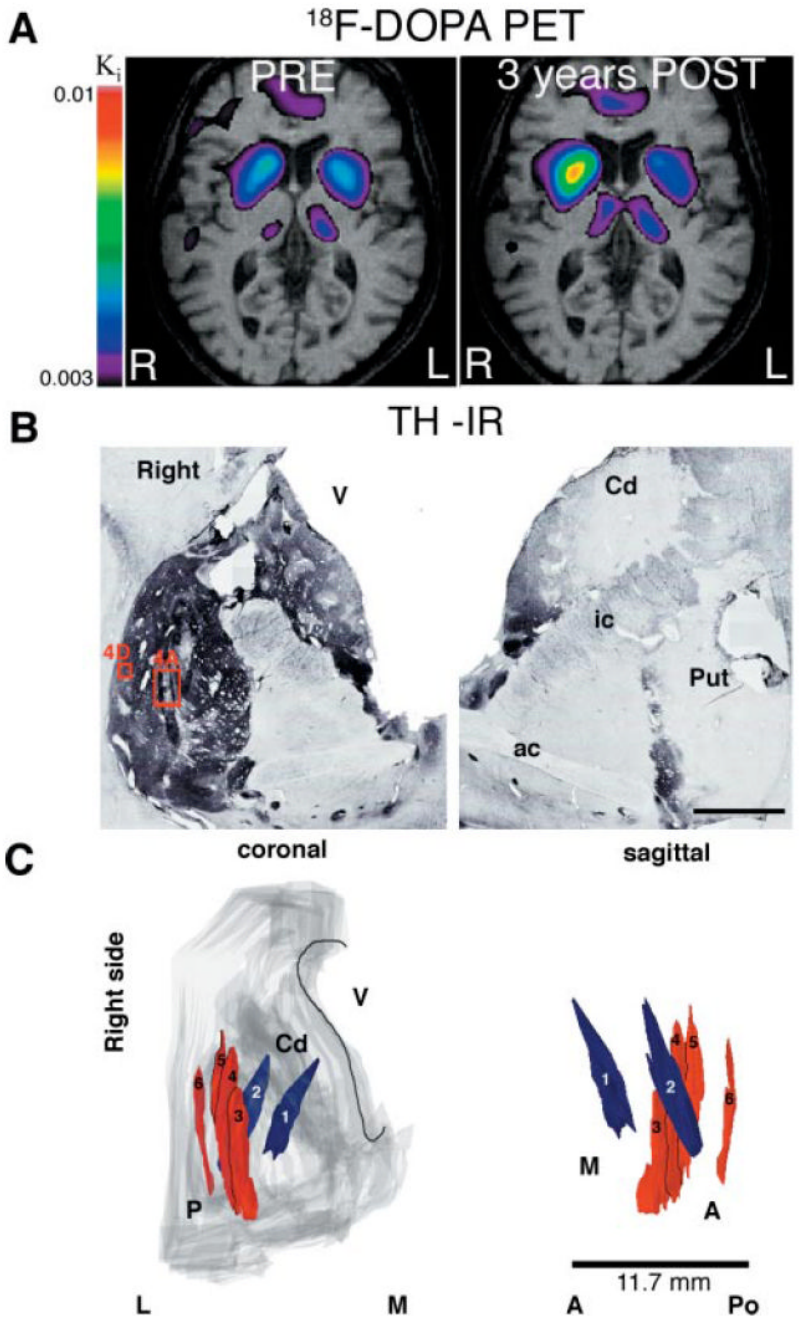

Fig. 3.

(**A**) Parametric maps of F-DOPA uptake (Ki) overlaid on the second patient's MRI before and 3 years after transplantation. Note the marked increase in ^{18}F-DOPA uptake in the right putamen (>200%) while the loss progressed during this time period on the left side (45% loss) (Ki values are shown in Table 1B). (**B**) Macroscopic aspect of TH immunoreactivity at the level of the anterior commissure in the second patient. The right putamen was completely reinnervated by the TH neurons distributed in the six tracks (see schematic reconstruction in **C**) at this anatomical level. No surviving TH neurons were found in the left putamen (which received only one deposit), corresponding to *in vivo* data; partial volume effect and resolution of the PET precludes direct quantitative comparison between the histological and imaging

studies. (**C**) 3D reconstruction of the six tracks in the right putamen. Numbers 1 and 2 followed a tangential direction from caudate to putamen; 3–6 are parallel (numbered anterior to posterior) to the major axis of the putamen. P = putamen; Cd = caudate nucleus; V = lateral ventricle; A = anterior; Po = posterior; M = medial; L = lateral. The boxed areas in **B** are shown at higher magnification in Fig. 4A and 4D. Scale bar in **B**, 1 cm.

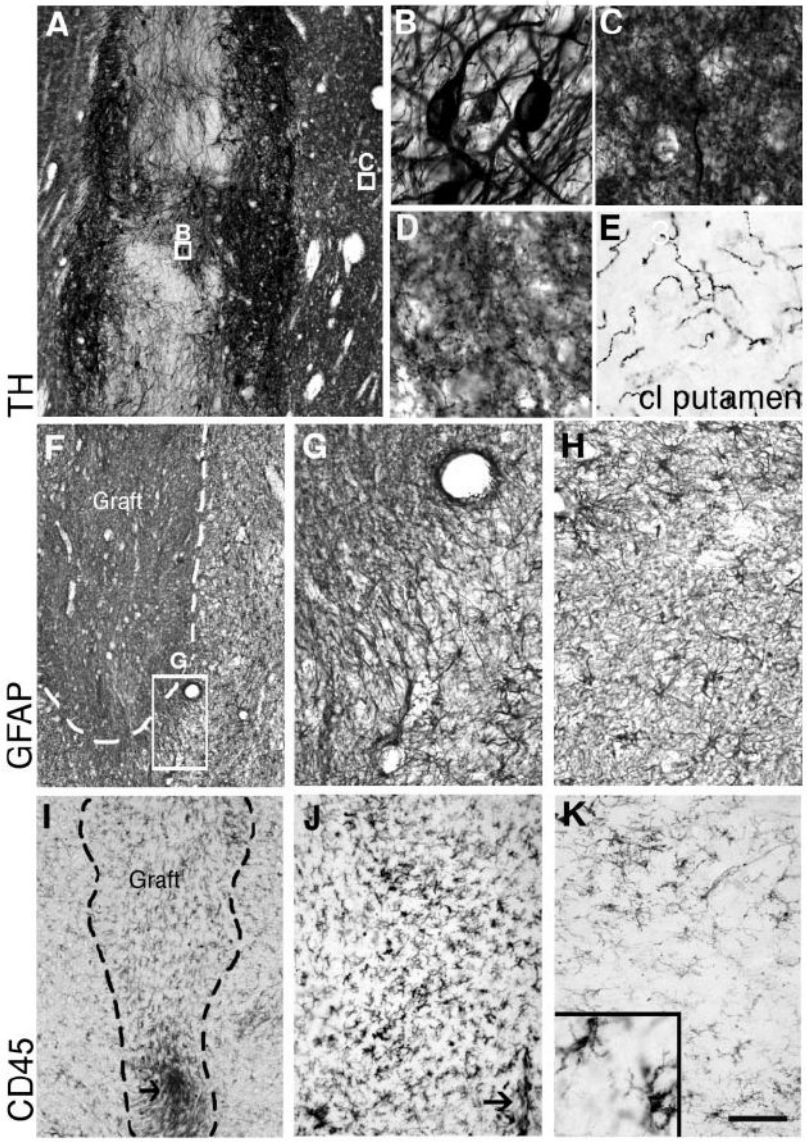

Fig. 4.

TH immunostaining of one of the transplants located in the right putamen of patient 2 showing the dense neurite outgrowth into the host putamen (central boxed area in Fig. 3B). Within the graft (**B**, boxed in **A**), TH-positive neurites from grafted neurons were thick and scarcely branched, while around the graft (**C**, boxed area in **A**), and further away (**D**, area shown boxed in Fig. 3B) they formed a dense network of fine branches approaching normal innervation in some areas of the putamen. Compare the fibre density with the contralateral putamen (**E**), where there was no graft survival. (**F**,**G**) GFAP immunostainings showing a representative transplant located in the putamen of patient 2. (**F**–**H**) Astroglial density was not increased in the graft core but around the graft deposits there was a band of variable thickness (<1 mm) of fibrous hypertrophic astrocytes (**G**, boxed in **F**). Further away, the astrocytic density and morphology were similar to those of normal striatum (**H**; illustrates a similar area from the putamen of patient 1). Microglial cells were identified by immunoreactivity against CD45 (common leucocyte antigen, CLA) and CD68 (activated microglia, not shown). (**I**–**J**) Representative microphotographs of CD45 immunostaining showing a local circumscribed increase in microglial cell density around needle tracks (arrows), which was very similar for all the grafts

located in the putamen in patient 1 (shown in **I**) and in both the midbrain and the striatal deposits in patient 2. At higher magnification (**J**) a few macrophages could be observed along the needle track (arrow), but most microglial cells showed a typical resting branched morphology (see detail in the inset in **K**) comparable to that observed in striatal regions at a distance (away) from the grafts (**K**). Scale bar: **A**, 500 μm; **F**, **I**, 400 μm; **G**,**H**,**J**,**K**, 200 μm; **C**–**E** and inset in **K**, 75 μm; **B**, 25 μm.

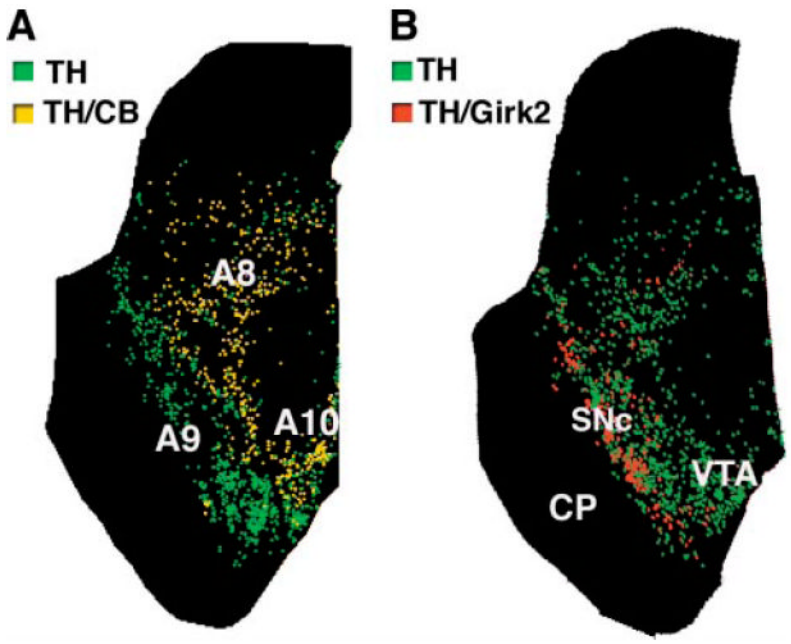

Fig. 5.

Distribution of subpopulations of DA neurons in human control midbrain. Maps of TH-positive neurons and their coexpression of calbindin (**A**) and Girk2 (**B**), two markers differentially expressed by Ventral mesencephalic DA neurons. Maps were generated from transverse serial sections double-immunolabelled for TH and each marker. Each dot represents a cell. (**A**) Calbindin/TH neurons, which are relatively spared in Parkinson's disease, are located in medial and dorsal regions and not found in ventral SNc. (**B**) Girk2/TH neurons are predominantly located in the ventral tier of the SNc, the most vulnerable region in Parkinson's disease. A8 = retrorubral area; A9 = substantia nigra; A10 = ventral tegmental area; CP = cerebral peduncle; RN = red nucleus; SNc = substantia nigra pars compacta; VTA = ventral tegmental area.

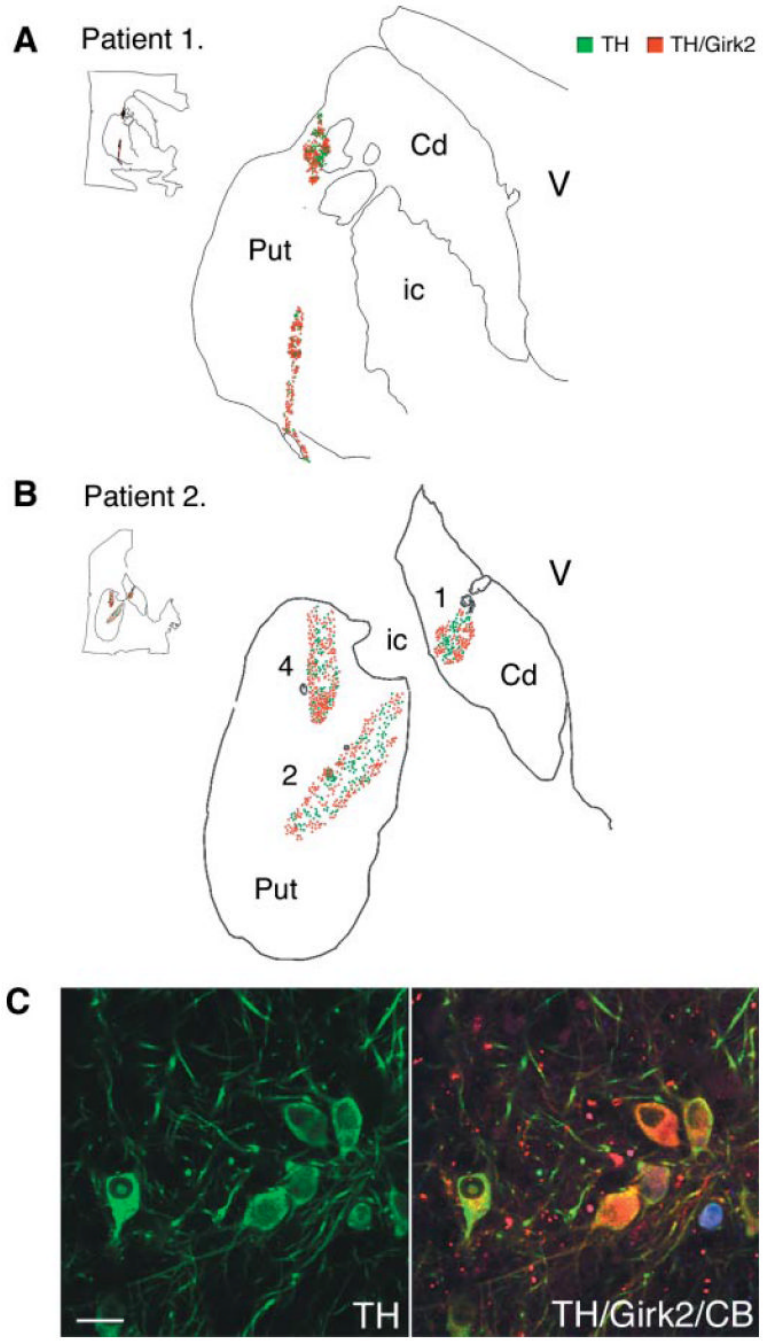

Fig. 6.

Maps of the dopamine subpopulations, TH/Girk2-positive neurons (red) and TH/Girk2-negative neurons (green) in the putaminal grafts. The maps were generated from representative transverse sections double-immunolabelled for TH and Girk2 using Neurolucida software. Each dot represents one cell. (**A**, patient 1, and **B**, patient 2) TH/Girk2-positive neurons were preferentially located in the outer layer of the grafts in the putaminal grafts. (**C**) Confocal images of triple immunofluorescence studies of TH (green), Girk2 (red) and calbindin (blue) within a putaminal graft (see Table 2 for quantification). Numbers identified the tracks as described in Fig. 3. TH = tyrosine hydroxylase; CB = calbindin; Cd = caudate; Put = putamen; V = lateral ventricle; ic = internal capsule. Scale bar in **C**, 50 μm.

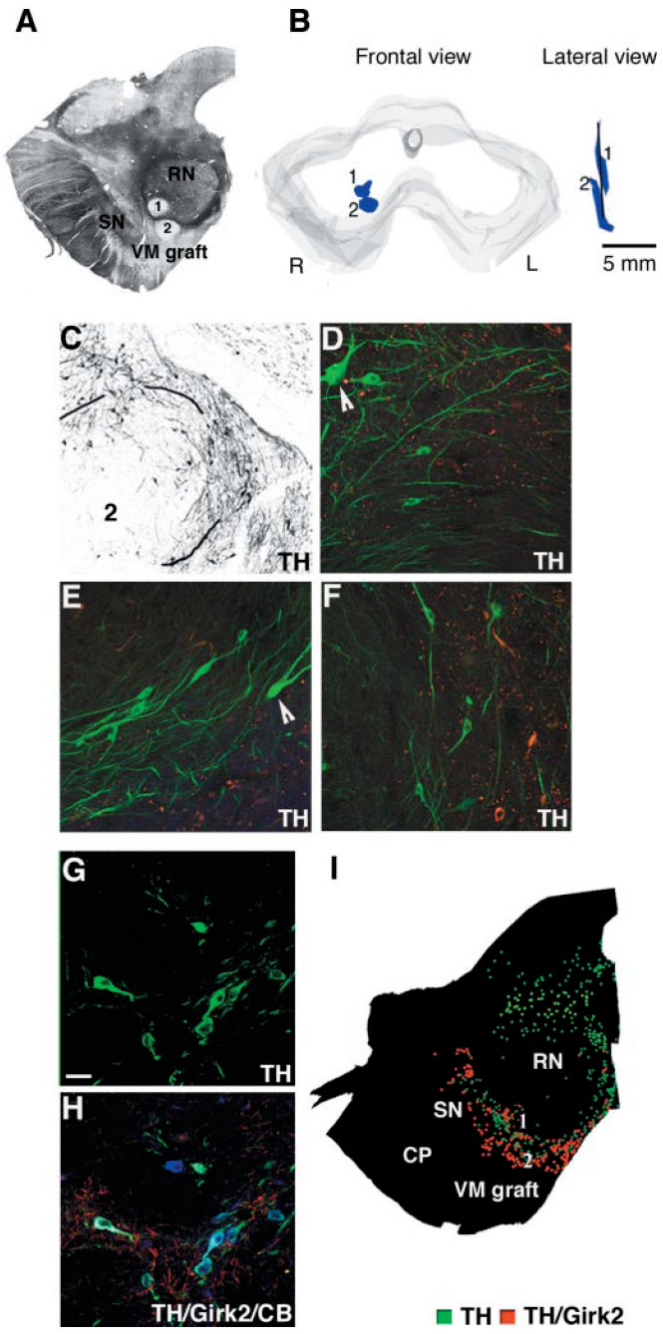

Fig. 7.

Midbrain graft. (**A**) Brightfield photograph of a representative unstained section showing the two nigral deposits identified in the right midbrain, at the border between the red nucleus and the rostral part of the SN. (**B**) Schematic representation of the stereological 3D reconstruction of the grafts in the right midbrain. At this level two parallel deposits were found between the red nucleus and the rostral SN, spanning 6.5 mm along the rostrocaudal axis. (**C**–**F**) TH immunostaining showed a typical disposition of transplanted neurons in the periphery of the graft. There were fewer TH neurons (Table 2) than in the striatal deposits and limited outgrowth. Higher magnification of three areas in this same deposit showing the small TH neurons within the graft where there is no lipofuscin (reddish deposits in the microphotograph).

Arrows in **D** and **E** point to host neurons which are bigger and heavily melanized. (**G**–**H**) Confocal images of TH neurons in the graft. Some TH neurons coexpressed Girk2 and calbindin (colours as in Fig. 3) (Table 2). (**I**) Two dopamine subpopulations TH-positive/Girk2-positive (red) and TH-positive/Girk2-negative (green) were mapped in the mesencephalon of this patient at the level of the red nucleus (graft location), showing a high expression of Girk2 except in the midline populations. Around 50% of TH cells in the midbrain grafts coexpressed Girk2 (Table 2). In the mapped sections there was no preferential distribution of the TH/Girk2 (red) population in the margins of the deposits. Scale bar: **C**, 150 μm; **D**–**H**, 50 μm.

Table 1

A Functional outcome 3 years after transplantation: patient 1

Measure	Baseline	3 years after transplantation	Change
UPDRS			
Motor			
Off	50	23	54%
On	30	16	47%
Total			
Off	97	67	31%
On	78	58	25%
Dyskinesia scores	12	8	34%
% time in Off	50%	25%	50%
Pro/sup			
Right			
Off	15	23	53%
On	19	24	26%
Left			
Off	14	23	64%
On	15	22	47%
[^{18}F] fluorodopa K_i			
Right putamen	0.00174	0.007068 (28 months)	306%
Left putamen	0.003355	0.005205 (28 months)	98%

B Functional outcome 3 years after transplantation: patient 2

Measure	Baseline	3 years after transplantation	Change
UPDRS			
Motor			
Off	84	44	48%
On	42	33	22%
Total			
Off	155	84	46%
On	102	73	28%
Dyskinesia scores	23	2	91%
% time in Off	50%	25%	50%
Pro/sup			
Right			
Off	5	7	40%
On	26	19	−27%
Left			
Off	8	23	187%
On	22	22	0%
[^{18}F] fluorodopa K_i			
Right putamen	0.001578	0.005088	222%
Left putamen	0.003493	0.001898	−45%
Right midbrain	0.001827	0.003474	90%
Left midbrain	0.002467	0.003025	22%

Table 2

Stereological and phenotypic analyses of the dopamine subpopulations in the transplants

Patient	Total graft volume (mm^3)	Total TH^+ cells	$TH^+CB^+Girk2^-$ (%)	$TH^+CB^-Girk2^+$ (%)	$TH^+CB^-Girk2^-$ (%)	$TH^+CB^+Girk2^+$ (%)
1						
Right putamen	71.12	127 189	15	39	14	32
Left putamen	41.42	98 913	23	44	8	25
2						
Right striatum	128.29	202 933	8	50	25	18
Right midbrain	20.8	4289	22	21	30	27